

# Knowledge Transfer via Multi-Head Feature Adaptation for Whole Slide Image Classification

Conghao Xiong<sup>1</sup>, Yi Lin<sup>2</sup>, Hao Chen<sup>2,3</sup>, Joseph Sung<sup>4</sup>, and Irwin King<sup>1</sup>

<sup>1</sup> Department of Computer Science and Engineering,  
The Chinese University of Hong Kong, HKSAR  
chxiong21@cse.cuhk.edu.hk

<sup>2</sup> Department of Computer Science and Engineering,  
The Hong Kong University of Science and Technology, HKSAR

<sup>3</sup> Department of Chemical and Biological Engineering,  
The Hong Kong University of Science and Technology, HKSAR

<sup>4</sup> Lee Kong Chian School of Medicine, Nanyang Technological University, Singapore

**Abstract.** Transferring prior knowledge from a source domain to the same or similar target domain can greatly enhance the performance of models on the target domain. However, it is challenging to directly leverage the knowledge from the source domain due to task discrepancy and domain shift. To bridge the gaps between different tasks and domains, we propose a Multi-Head Feature Adaptation module, which projects features in the source feature space to a new space that is more similar to the target space. Knowledge transfer is particularly important in Whole Slide Image (WSI) classification since the number of WSIs in one dataset might be too small to achieve satisfactory performance. Therefore, WSI classification is an ideal testbed for our method, and we adapt multiple knowledge transfer methods for WSI classification. The experimental results show that models with knowledge transfer outperform models that are trained from scratch by a large margin regardless of the number of WSIs in the datasets, and our method achieves state-of-the-art performances among other knowledge transfer methods on multiple datasets, including TCGA-RCC, TCGA-NSCLC, and Camelyon16 datasets.

**Keywords:** Whole Slide Image Classification · Knowledge Transfer

## 1 Introduction

Deep learning is the de facto method in computer vision [10, 21, 29, 31] and Whole Slide Image (WSI) classification, such as breast [19], prostate [3], skin [13], pancreas [17] and lung cancer [5], *etc.* However, for some diseases, the patient cohort is small, limiting the total number of WSIs in the dataset [2]. Furthermore, WSIs are gigapixel images and it takes several hours for a pathologist to annotate one single WSI, which is labour-extensive and expensive. Hence, the number of WSIs can be insufficient, resulting in an unsatisfactory performance of the model.

Transfer learning, which transfers prior knowledge in a pre-trained model (teacher model) obtained from a source domain to the model (student model) on

a target domain, is one of the feasible ways to tackle the data insufficiency problem [21,31]. The most frequently-used transfer learning method is fine-tuning, which initialises the student model with weights from a teacher model. Also, feature transfer is another option, which transfers the features into a new feature space [14]. Most methods for WSI classification only use the models pre-trained on ImageNet to extract features from patches [16,23,24].

However, transfer learning faces the challenges of task discrepancy and domain shift. The tasks of the source domain and target domain can be quite different. For instance, the tasks of **The Cancer Genome Atlas** (TCGA) datasets can be cancer subtyping, survival prediction, *etc.*, while that of Camelyon16 [18] is to detect metastases. Also, differences between domains can be significant. First, tumour regions of Camelyon16 only take up less than 10% of the WSIs, while they can account for 80% in TCGA datasets. Second, different institutions might have different staining materials, leading to tone differences in the WSIs.

Adding a projection head, *i.e.*, feature transfer, is one viable way of solving these problems [4,8]. Direct supervision is “hard supervision” that outputs from the teacher model are unchangeable. In contrast, adding a projection head is “soft supervision” that allows slight errors. The projection head maps features from the teacher model (teacher features) to another feature space that has less distinction with the target feature space, in which way the teacher knowledge can be more accurately transferred to the student model. We propose a **Multi-Head Feature Adaptation** (MHFA) module that follows this path and utilises **Multi-Head Attention** (MHA) [25,26] to fully exploit new patterns and combinations that are closer to the target space. Besides the data insufficiency scenario, Our method also provides consistent improvements when the data is abundant.

Additionally, we also investigate knowledge distillation, which transfers knowledge from a large teacher model to a smaller student model on the same dataset [1,6,9,11,27]. Given the fact that the sizes of the new models are growing [7,22,28], knowledge distillation compresses large models to smaller ones so that users with limited computational resources can also achieve comparable performances. Our method is also applicable to knowledge distillation since transfer learning and knowledge distillation can be formulated under knowledge transfer [1].

1. We propose an MHFA module to project the teacher features to another space so that the gaps between different tasks and domains can be bridged.
2. We adapt multiple knowledge transfer methods for WSI classification to overcome the data insufficiency problem by leveraging prior knowledge.
3. We conduct extensive experiments on multiple datasets, including TCGA-RCC, TCGA-NSCLC and Camelyon16. The experimental results show that our method outperforms other methods consistently.

## 2 Methodology

### 2.1 Knowledge Transfer Formulation

**Preliminary Definitions.** A domain  $\mathcal{D} = (\mathcal{X}, P(\mathbf{X}))$  consists of a feature space  $\mathcal{X}$  and a marginal probability distribution  $P(\mathbf{X})$ , where  $\mathbf{X} = \{\mathbf{x}_1, \dots, \mathbf{x}_n\} \in \mathcal{X}$ .

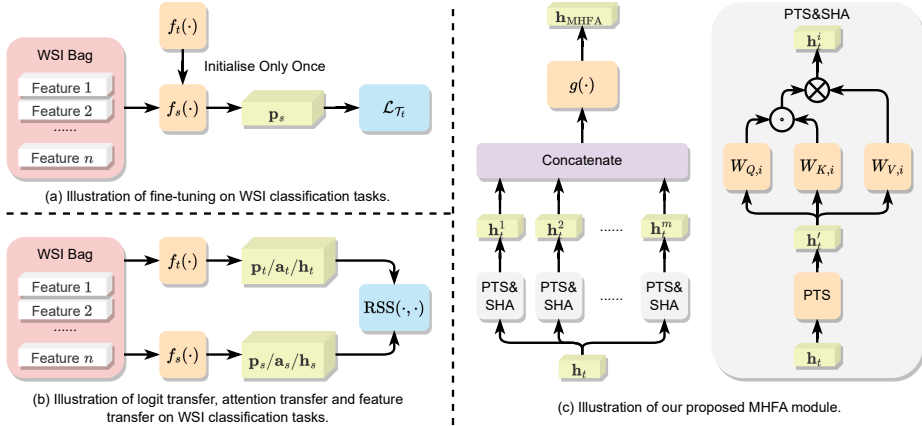


**Fig. 1.** Illustrations of knowledge transfer techniques and our MHFA module.  $f_t(\cdot)$  is the teacher model trained on  $\mathcal{D}_s$  and  $f_s(\cdot)$  is the student model on  $\mathcal{D}_t$ .

A task  $\mathcal{T} = (\mathcal{Y}, f(\cdot))$  is also comprised of two components: the corresponding label collection  $\mathcal{Y}$  and the objective predictive function  $f(\cdot) : \mathcal{X} \rightarrow \mathcal{Y}$ .

**Knowledge Transfer.** Considering the source and target domains  $\mathcal{D}_s, \mathcal{D}_t$  and the tasks on the two domains  $\mathcal{T}_s, \mathcal{T}_t$  with teacher model  $f_t(\cdot)$  trained and student model  $f_s(\cdot)$  untrained, knowledge transfer utilises  $f_t(\cdot)$  from the source domain to enhance the objective predictive function at the target domain  $f_s(\cdot)$ . Furthermore, if  $\mathcal{D}_s \neq \mathcal{D}_t$  or  $\mathcal{T}_s \neq \mathcal{T}_t$ , this is the transfer learning scenario, and if  $\mathcal{D}_s = \mathcal{D}_t, \mathcal{T}_s = \mathcal{T}_t$  and  $f_t(\cdot)$  is more complex than  $f_s(\cdot)$ , it is the knowledge distillation scenario. The goal of this work is to investigate knowledge transfer methods applicable to both transfer learning and knowledge distillation.

## 2.2 Knowledge Transfer Framework for WSI Classification

The overview of the knowledge transfer framework is shown in Fig. 1. Given the teacher model  $f_t(\cdot)$  trained on  $\mathcal{D}_s$  with  $\mathcal{T}_s$ , knowledge transfer delivers the knowledge acquired in  $f_t(\cdot)$  to the student model  $f_s(\cdot)$  on  $\mathcal{D}_t$  with  $\mathcal{T}_t$ . In this work, we study four knowledge transfer techniques for WSI classification.

**Fine-tuning.** Initialisation has significant impacts on neural network training. Models that are initialised with pre-trained weights on related datasets tend to converge faster and achieve better performance. Hence, fine-tuning, meaning that the model is first initialised with a pre-trained model and then trained on the target dataset, is a popular method since the preliminary knowledge from the source dataset can greatly facilitate the training on the target dataset.

**Logit Transfer.** Logits are the predicted probability distribution of the labels. Logits from a well-trained teacher model  $\mathbf{p}_t \in \mathbb{R}^{1 \times c}$ , where  $c$  is the number of classes, can enhance the student model [12] by pulling the logits of the student model  $\mathbf{p}_s \in \mathbb{R}^{1 \times c}$  closer to  $\mathbf{p}_t$ , since  $\mathbf{p}_t$  can serve as pseudo-labels for  $\mathbf{p}_s$ .

**Attention Transfer.** Under the MIL setting, the WSIs are divided into patches and the importance of each patch can differ. The attention map indicates the significance of each patch, and it can be easily derived from attention-based MIL models. Therefore, assume the number of patches is  $n$ , pulling the attention maps  $\mathbf{a}_s \in \mathbb{R}^{1 \times n}$  of the student model closer to those of the teacher model  $\mathbf{a}_t \in \mathbb{R}^{1 \times n}$  helps the student model learn the most discriminative regions [30].

**Feature Transfer.** The bag features that are decisive for the prediction can be used as the supervision signal to improve the bag representation of the student model  $\mathbf{h}_s \in \mathbb{R}^{1 \times d_s}$  under the guidance of the bag representation from the teacher model  $\mathbf{h}_t \in \mathbb{R}^{1 \times d_t}$ . In some scenarios like knowledge distillation,  $d_t$  is typically larger than  $d_s$ . Therefore, dimension reduction techniques, such as singular value decomposition and principal component analysis, are often required [11].

In summary, the loss functions for these methods are given in Eq. (1) as,

$$\mathcal{L} = \begin{cases} \alpha \text{RSS}(\mathbf{p}_t, \mathbf{p}_s) + \mathcal{L}_{\mathcal{T}_t}, & \text{logit transfer,} \\ \alpha \text{RSS}(\mathbf{a}_t, \mathbf{a}_s) + \mathcal{L}_{\mathcal{T}_t}, & \text{attention transfer,} \\ \alpha \text{RSS}(\mathbf{h}_t, \mathbf{h}_s) + \mathcal{L}_{\mathcal{T}_t}, & \text{feature transfer,} \end{cases} \quad (1)$$

where RSS is the **R**esidual **S**um of **S**quares (RSS) loss,  $\alpha$  is a coefficient, and  $\mathcal{L}_{\mathcal{T}_t}$  is the classification loss function of  $\mathcal{T}_t$ .

### 2.3 Multi-Head Feature Adaptation Module

We adopt feature-based knowledge transfer in our work, as it is well-suited to both transfer learning and knowledge distillation. To address the task discrepancy and domain shift problems, we propose an MHFA module, which projects the teacher feature  $\mathbf{h}_t \in \mathbb{R}^{1 \times d_t}$  to a new feature  $\mathbf{h}_{\text{MHFA}} \in \mathbb{R}^{1 \times d_s}$ . Therefore, the loss function for our method can be expressed in Eq. (2) as,

$$\mathcal{L} = \alpha \text{RSS}(\mathbf{h}_{\text{MHFA}}, \mathbf{h}_s) + \mathcal{L}_{\mathcal{T}_t}. \quad (2)$$

First, it normalises the teacher feature vectors using **P**ower **T**emperature **S**caling (PTS) normalisation function [11], which is given in Eq. (3) as,

$$\mathbf{h}'_t = \text{PTS}(\mathbf{h}_t) = \text{sign}(\mathbf{h}_t) \left| \frac{\mathbf{h}_t}{T} \right|^{\frac{1}{t}} \in \mathbb{R}^{1 \times d_t}, \quad (3)$$

where  $T = 0.1$  and  $t = 3$  as stated in [11],  $\text{sign}(\cdot)$  is the sign function.

Then the MHA module [25] is applied on the normalised teacher feature vector  $\mathbf{h}'_t$  to discover new patterns and combinations of it. The MHA module can be expressed in Eq. (4) as,

$$\mathbf{H}_t = \text{MHA}(\mathbf{h}'_t, m) = \text{concat}(\text{SHA}_1(\mathbf{h}'_t), \dots, \text{SHA}_m(\mathbf{h}'_t)) \in \mathbb{R}^{m \times d_s}, \quad (4)$$

where  $\text{concat}(\cdot, \dots, \cdot)$  is the concatenation operation,  $m$  is the number of attention heads,  $d_s$  is the dimension of the student feature, and  $\text{SHA}_i(\cdot)$  is the  $i$ -th **S**ingle-**H**ead **A**ttention (SHA) module [25], which is defined in Eq. (5) as,

$$\text{SHA}_i(\mathbf{h}'_t) = \frac{(\mathbf{h}'_t \mathbf{W}_{Q,i}) \cdot (\mathbf{h}'_t \mathbf{W}_{K,i})^T}{\sqrt{d_t}} (\mathbf{h}'_t \mathbf{W}_{V,i}) \in \mathbb{R}^{1 \times d_s}, \quad (5)$$

where  $\mathbf{W}_{Q,i}, \mathbf{W}_{K,i} \in \mathbb{R}^{d_t \times d_k}, \mathbf{W}_{V,i} \in \mathbb{R}^{d_t \times d_s}$  are three learnable matrices.

Finally, we utilised the gated attention mechanism  $g(\cdot)$  [15] to assign importance scores to the features  $\mathbf{H}_t$ . These features are useful to different extents, and the purpose of the gated attention mechanism is to find the most decisive ones. The gated attention mechanism is given in Eq. (6) as,

$$g(\mathbf{H}_t) = ((\text{softmax}(\tanh(\mathbf{H}_t \mathbf{W}_V) \odot \sigma(\mathbf{H}_t \mathbf{W}_U))) \mathbf{w})^T \mathbf{H}_t \in \mathbb{R}^{1 \times d_s}, \quad (6)$$

where  $\tanh(\cdot)$  is the tanh function,  $\sigma(\cdot)$  is the sigmoid function,  $\mathbf{w} \in \mathbb{R}^{d' \times 1}$ ,  $\mathbf{W}_V, \mathbf{W}_U \in \mathbb{R}^{d_s \times d'}$  are the learnable matrices and  $d'$  is the hidden dimension of the gated attention mechanism. Combining all three steps mentioned above, the final supervision feature from the teacher model  $\mathbf{h}_{\text{MHFA}}$  is given in Eq. (7) as,

$$\mathbf{h}_{\text{MHFA}} = \text{MHFA}(\mathbf{h}_t, m) = g(\text{MHA}(\text{PTS}(\mathbf{h}_t), m)). \quad (7)$$

### 3 Experiments and Results

#### 3.1 Dataset Descriptions

**Camelyon16.** [18] There are 399 WSIs of lymph nodes with and without metastasis in women breast cancer tissues. The training and test datasets contain 270 and 129 WSIs, respectively. We split the training dataset into training and validation datasets by 8:2 and compare the performances on the official test dataset. **TCGA-RCC**<sup>5</sup>. There are 940 WSI slides in this dataset. It consists of 121 WSIs from 109 cases in Kidney Chromophobe Renal Cell Carcinoma (TCGA-KICH), 519 WSIs from 513 cases in Kidney Renal Clear Cell Carcinoma (TCGA-KIRC), and 300 WSIs from 276 cases in Kidney Renal Papillary Cell Carcinoma (TCGA-KIRP). The dataset is split into training, validation, and test datasets by the ratio of 6:1.5:2.5, respectively.

**TCGA-NSCLC.** There are 1,053 WSI slides in this dataset. It consists of 512 WSIs from 478 cases in Lung Squamous Cell Carcinoma (TCGA-LUSC), and 541 WSIs from 478 cases in Lung Adenocarcinoma (TCGA-LUAD). The dataset split is the same as TCGA-RCC dataset.

#### 3.2 Implementation Details

**Evaluation Metrics.** Area Under the Curve (AUC), F1 and accuracy are the evaluation metrics. These metrics can holistically reflect the performances of the models. The thresholds of F1 and accuracy scores are set to 0.5.

**Training Settings.** The baseline knowledge transfer methods include (1) no knowledge transfer, (2) fine-tuning, (3) Logit Transfer (LT) [12], (4) Attention Transfer (AT) [30] and (5) PTS norm [11]. The MIL model in our method is initialised with the teacher model when possible. The base models are CLAM

<sup>5</sup> The results shown here are in whole or part based upon data generated by the TCGA Research Network: <https://www.cancer.gov/tcga>

**Table 1.** Results on Camelyon16 with teacher and student models being CLAM S, and source domains being TCGA-RCC and TCGA-NSCLC. RCC→Camelyon16 column contains performances of the student model trained on Camelyon16 and the teacher model trained on TCGA-RCC. The best results are in red bold, and the second best ones are in blue underline. The subscript in each cell is the standard derivation. Our method is highlighted with light cyan.

METHOD	RCC→Camelyon16			NSCLC→Camelyon16		
	AUC↑	F1↑	Accuracy↑	AUC↑	F1↑	Accuracy↑
CLAM S [20]	0.847 <sub>0.035</sub>	0.789 <sub>0.037</sub>	0.819 <sub>0.030</sub>	0.847 <sub>0.035</sub>	0.789 <sub>0.037</sub>	0.819 <sub>0.030</sub>
Fine-tuning	<u>0.880</u> <sub>0.021</sub>	<u>0.850</u> <sub>0.025</sub>	<u>0.868</u> <sub>0.021</sub>	<u>0.894</u> <sub>0.005</sub>	<u>0.835</u> <sub>0.014</sub>	<u>0.855</u> <sub>0.009</sub>
AT [30]	0.844 <sub>0.010</sub>	0.793 <sub>0.027</sub>	0.819 <sub>0.024</sub>	0.848 <sub>0.013</sub>	0.787 <sub>0.030</sub>	0.817 <sub>0.024</sub>
PTS norm [11]	0.858 <sub>0.031</sub>	0.830 <sub>0.043</sub>	0.848 <sub>0.039</sub>	0.778 <sub>0.007</sub>	0.781 <sub>0.015</sub>	0.809 <sub>0.009</sub>
Ours	<b>0.910</b> <sub>0.006</sub>	<b>0.867</b> <sub>0.003</sub>	<b>0.879</b> <sub>0.004</sub>	<b>0.899</b> <sub>0.027</sub>	<b>0.852</b> <sub>0.023</sub>	<b>0.871</b> <sub>0.018</sub>

**Table 2.** Results on TCGA-RCC and TCGA-NSCLC with teacher and student models being CLAM S.

METHOD	RCC→NSCLC			NSCLC→RCC		
	AUC↑	F1↑	Accuracy↑	AUC↑	F1↑	Accuracy↑
CLAM S [20]	0.934 <sub>0.007</sub>	0.863 <sub>0.008</sub>	0.863 <sub>0.008</sub>	0.973 <sub>0.004</sub>	0.866 <sub>0.009</sub>	0.892 <sub>0.009</sub>
Fine-tuning	0.936 <sub>0.005</sub>	0.863 <sub>0.004</sub>	0.863 <sub>0.004</sub>	0.974 <sub>0.002</sub>	<u>0.886</u> <sub>0.005</sub>	<u>0.905</u> <sub>0.002</sub>
AT [30]	0.946 <sub>0.006</sub>	0.876 <sub>0.018</sub>	0.876 <sub>0.018</sub>	<u>0.975</u> <sub>0.003</sub>	0.869 <sub>0.004</sub>	0.896 <sub>0.002</sub>
PTS norm [11]	<u>0.949</u> <sub>0.004</sub>	<u>0.878</u> <sub>0.010</sub>	<u>0.878</u> <sub>0.010</sub>	0.970 <sub>0.002</sub>	0.877 <sub>0.015</sub>	0.887 <sub>0.012</sub>
Ours	<b>0.953</b> <sub>0.004</sub>	<b>0.886</b> <sub>0.008</sub>	<b>0.886</b> <sub>0.008</sub>	<b>0.980</b> <sub>0.001</sub>	<b>0.897</b> <sub>0.017</sub>	<b>0.913</b> <sub>0.014</sub>

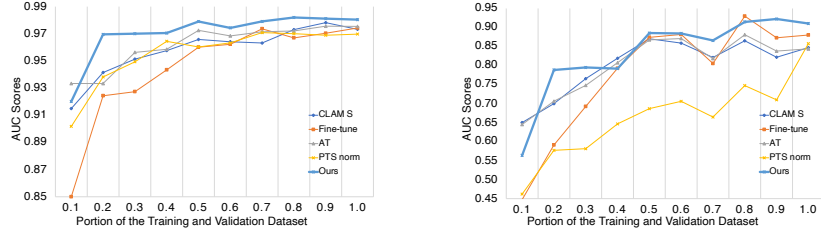
Small, CLAM Big [20]. The model with the lowest validation loss is chosen for inference on the test dataset and the result of that is reported. The model training is ceased when the validation loss stops decreasing for 20 epochs. We run the models three times and the average performances are reported.

**Hyper-parameters.** The learning rate and weight decay are set to 2e-4 and 1e-5. The Adam optimizer is used. Dropout is set to 0.25 for CLAM S and B. The coefficient  $\alpha$  is set to 0.1. The number of attention head  $m$  is 8. The WSIs are split into  $256 \times 256$  non-overlapping patches at level 1 resolution ( $20 \times$ ). ResNet-50 [10] pre-trained on ImageNet is used to extract features from the patches.

### 3.3 Comparison with Related Methods

We compare our method with other methods in the following settings: (1) transfer learning, (2) transfer learning in low-resource settings, (3) knowledge distillation, (4) knowledge distillation and transfer learning.

**Transfer Learning.** The results are shown in Table 2 and Table 1. Our proposed method achieves the best performance across all metrics, especially on Camelyon16, where our method outperforms other methods by a large margin,



(a) AUC Scores on TCGA-RCC dataset. (b) AUC Scores on Camelyon16 dataset.

**Fig. 2.** Comparison of different knowledge transfer methods on the TCGA-RCC and Camelyon16 datasets of different sizes. The curves for our method are in bold.

demonstrating the effectiveness of our method. Furthermore, due to the areas of tumour regions, Camelyon16 is more difficult than TCGA datasets. The experimental results further prove that our method can effectively transfer knowledge from a simpler dataset to a harder one. Comparing these two tables, methods with additional supervision signals perform better within TCGA dataset transfer, and fine-tuning performs better when transferring knowledge from TCGA datasets to Camelyon16 dataset. The reason for this is that tasks and domains for TCGA datasets are more similar. Methods with additional supervision signals actually all rely on the attention scores since both bag features and logits are derived from the attention scores. Furthermore, the areas of the tumour regions are drastically different between Camelyon16 and TCGA datasets, leading to different attention distributions. Therefore, attention-derived methods may consistently introduce bias, resulting in lower performance compared to fine-tuning.

**Transfer Learning in Low Resource Settings.** One of the essential applications for knowledge transfer is to transfer the knowledge acquired in a large dataset to the model in a smaller dataset. To make the experiments easier, we choose to only consider transfer learning without knowledge distillation. We create new training and validation datasets with varying sizes and the test dataset remains the same. The experimental results are shown in Fig. 2. Generally, for every method, the larger the dataset is, the better the performance will be. Our method achieved the best performance in most of these experiments. On extremely low resource settings, CLAM S has competitive AUC scores, but not so when the dataset gets larger. AT performs particularly well in low-resource settings for TCGA-RCC dataset, but has similar performances as CLAM S on Camelyon16. PTS norm is not a competitive method in low-resource settings.

**Knowledge Distillation.** Fine-tuning is no longer valid since the model architectures are different. Instead, since the source and target datasets are the same, logit transfer becomes feasible. The results of the experiments are shown in Table 3. Overall, most methods provide improvements compared to CLAM S. Our method improves the AUC score on TCGA-RCC dataset by 0.7%, and 1.9% on TCGA-NSCLC dataset. PTS norm outperforms all other methods by a large margin on TCGA-NSCLC dataset. However, it is the only method that

**Table 3.** Results of knowledge distillation on TCGA-RCC and TCGA-NSCLC with teacher and student models being CLAM S and B.

METHOD	NSCLC			RCC		
	AUC↑	F1↑	Accuracy↑	AUC↑	F1↑	Accuracy↑
CLAM S [20]	0.934 <sub>0.007</sub>	0.863 <sub>0.008</sub>	0.863 <sub>0.008</sub>	0.973 <sub>0.004</sub>	0.866 <sub>0.009</sub>	0.892 <sub>0.009</sub>
CLAM B [20]	0.942 <sub>0.005</sub>	0.847 <sub>0.011</sub>	0.848 <sub>0.012</sub>	0.974 <sub>0.005</sub>	0.856 <sub>0.003</sub>	0.886 <sub>0.017</sub>
LT [12]	0.950 <sub>0.002</sub>	0.868 <sub>0.006</sub>	0.868 <sub>0.006</sub>	0.978 <sub>0.000</sub>	0.885 <sub>0.006</sub>	0.905 <sub>0.005</sub>
AT [30]	0.947 <sub>0.003</sub>	0.866 <sub>0.008</sub>	0.866 <sub>0.008</sub>	0.975 <sub>0.002</sub>	0.876 <sub>0.020</sub>	0.900 <sub>0.012</sub>
PTS norm [11]	0.962 <sub>0.003</sub>	0.894 <sub>0.004</sub>	0.894 <sub>0.004</sub>	0.964 <sub>0.005</sub>	0.853 <sub>0.003</sub>	0.877 <sub>0.009</sub>
Ours	0.953 <sub>0.001</sub>	0.885 <sub>0.002</sub>	0.885 <sub>0.002</sub>	0.980 <sub>0.001</sub>	0.880 <sub>0.006</sub>	0.900 <sub>0.005</sub>

**Table 4.** Results of knowledge distillation and transfer learning on TCGA-RCC and TCGA-NSCLC with teacher and student models being CLAM S and B.

METHOD	RCC→NSCLC			NSCLC→RCC		
	AUC↑	F1↑	Accuracy↑	AUC↑	F1↑	Accuracy↑
CLAM S [20]	0.934 <sub>0.007</sub>	0.863 <sub>0.008</sub>	0.863 <sub>0.008</sub>	0.973 <sub>0.004</sub>	0.866 <sub>0.009</sub>	0.892 <sub>0.009</sub>
CLAM B [20]	0.942 <sub>0.005</sub>	0.847 <sub>0.011</sub>	0.848 <sub>0.012</sub>	0.974 <sub>0.005</sub>	0.856 <sub>0.003</sub>	0.886 <sub>0.017</sub>
AT [30]	0.948 <sub>0.010</sub>	0.868 <sub>0.011</sub>	0.868 <sub>0.011</sub>	0.970 <sub>0.001</sub>	0.864 <sub>0.004</sub>	0.887 <sub>0.007</sub>
PTS norm [11]	0.949 <sub>0.002</sub>	0.882 <sub>0.004</sub>	0.882 <sub>0.004</sub>	0.970 <sub>0.001</sub>	0.883 <sub>0.009</sub>	0.899 <sub>0.005</sub>
Ours	0.951 <sub>0.005</sub>	0.874 <sub>0.008</sub>	0.875 <sub>0.008</sub>	0.981 <sub>0.001</sub>	0.888 <sub>0.013</sub>	0.906 <sub>0.011</sub>

does not enhance the original CLAM S on TCGA-RCC dataset. LT achieves the second-best AUC scores and the best F1 and accuracy scores on TCGA-RCC dataset. AT provides consistent improvements on both datasets.

**Knowledge Distillation and Transfer Learning.** Since the models and the datasets are both different, neither logit transfer nor fine-tuning is appropriate in this scenario. The results of the experiments are shown in Table 4. Our method again achieves the best performances across both datasets, demonstrating the efficacy of our method. Both PTS norm and AT do not enhance the performance on TCGA-RCC dataset under this setting, yet they provide 1.4% and 1.5% improvements on TCGA-NSCLC AUC scores, compared to CLAM S.

## 4 Conclusion

To address the task discrepancy and domain shift problems, we propose an MHFA module, which projects the teacher features to a new feature space that has less distinction with the target feature space, to discover new patterns and combinations of the teacher features. Our method achieves state-of-the-art performance among other adapted knowledge transfer methods, as evidenced by our experimental results. Besides, we adapt multiple knowledge transfer methods for WSI classification to improve the performance of the models and present

a benchmark for it. Our experimental results demonstrate that knowledge transfer significantly and consistently enhances the model performance compared to training from scratch regardless of the number of samples in the dataset.

## References

1. Ahn, S., Hu, S.X., Damianou, A.C., Lawrence, N.D., Dai, Z.: Variational information distillation for knowledge transfer. In: IEEE Conference on Computer Vision and Pattern Recognition, CVPR 2019, Long Beach, CA, USA, June 16-20, 2019. pp. 9163–9171. Computer Vision Foundation / IEEE (2019)
2. Aumpan, N., Vilaichone, R.k., Pornthisarn, B., Chonprasertsuk, S., Siramolpiwat, S., Bhanthumkomol, P., Nunanan, P., Issariyakulkarn, N., Ratana-Amornpin, S., Miftahussurur, M., Mahachai, V., Yamaoka, Y.: Predictors for regression and progression of intestinal metaplasia (im): A large population-based study from low prevalence area of gastric cancer (im-predictor trial). *PLOS ONE* **16**(8), 1–14 (08 2021)
3. Campanella, G., Hanna, M.G., Geneslaw, L., Miraflor, A., Werneck Krauss Silva, V., Busam, K.J., Brogi, E., Reuter, V.E., Klimstra, D.S., Fuchs, T.J.: Clinical-grade computational pathology using weakly supervised deep learning on whole slide images. *Nature Medicine* **25**(8), 1301–1309 (Aug 2019)
4. Caron, M., Touvron, H., Misra, I., Jégou, H., Mairal, J., Bojanowski, P., Joulin, A.: Emerging properties in self-supervised vision transformers. In: ICCV. pp. 9630–9640. IEEE (2021)
5. Chen, C.L., Chen, C.C., Yu, W.H., Chen, S.H., Chang, Y.C., Hsu, T.I., Hsiao, M., Yeh, C.Y., Chen, C.Y.: An annotation-free whole-slide training approach to pathological classification of lung cancer types using deep learning. *Nature Communications* **12**(1), 1193 (Feb 2021)
6. Chen, D., Mei, J., Zhang, H., Wang, C., Feng, Y., Chen, C.: Knowledge distillation with the reused teacher classifier. In: CVPR. pp. 11923–11932. IEEE (2022)
7. Chen, R.J., Chen, C., Li, Y., Chen, T.Y., Trister, A.D., Krishnan, R.G., Mahmood, F.: Scaling vision transformers to gigapixel images via hierarchical self-supervised learning. In: CVPR (2022)
8. Chen, T., Kornblith, S., Norouzi, M., Hinton, G.E.: A simple framework for contrastive learning of visual representations. In: ICML. Proceedings of Machine Learning Research, vol. 119, pp. 1597–1607. PMLR (2020)
9. Garg, A., Aggarwal, K., Saxena, M., Bhat, A.: Classifying Medical Histology Images Using Computationally Efficient CNNs Through Distilling Knowledge. In: Emerging Technologies in Data Mining and Information Security. pp. 713–721. Lecture Notes in Networks and Systems, Springer, Singapore (2021)
10. He, K., Zhang, X., Ren, S., Sun, J.: Deep residual learning for image recognition. In: CVPR (2016)
11. He, R., Sun, S., Yang, J., Bai, S., Qi, X.: Knowledge Distillation as Efficient Pre-training: Faster Convergence, Higher Data-efficiency, and Better Transferability. In: CVPR. pp. 9151–9161. IEEE, New Orleans, LA, USA (Jun 2022)
12. Hinton, G.E., Vinyals, O., Dean, J.: Distilling the knowledge in a neural network. *CoRR* **abs/1503.02531** (2015)
13. Ianni, J.D., Soans, R.E., Sankarapandian, S., Chamarthi, R.V., Ayyagari, D., Olsen, T.G., Bonham, M.J., Stavish, C.C., Motaparthi, K., Cockerell, C.J., Feeser,

T.A., Lee, J.B.: Tailored for Real-World: A Whole Slide Image Classification System Validated on Uncurated Multi-Site Data Emulating the Prospective Pathology Workload. *Scientific Reports* **10**(1), 3217 (Feb 2020)

14. III, H.D.: Frustratingly easy domain adaptation. In: *ACL* (2007)
15. Ilse, M., Tomczak, J., Welling, M.: Attention-based Deep Multiple Instance Learning. In: *ICML 2018*. PMLR (Jul 2018)
16. Kanavati, F., Tsuneki, M.: Breast Invasive Ductal Carcinoma Classification on Whole Slide Images with Weakly-Supervised and Transfer Learning. *Cancers* **13**(21), 5368 (Jan 2021), number: 21
17. Keikhosravi, A., Li, B., Liu, Y., Conklin, M.W., Loeffler, A.G., Eliceiri, K.W.: Non-disruptive collagen characterization in clinical histopathology using cross-modality image synthesis. *Communications Biology* **3**(1), 1–12 (Jul 2020)
18. Litjens, G., Bandi, P., Ehteshami Bejnordi, B., Geessink, O., Balkenhol, M., Bult, P., Halilovic, A., Hermens, M., van de Loo, R., Vogels, R., Manson, Q.F., Stathonikos, N., Baidoshvili, A., van Diest, P., Wauters, C., van Dijk, M., van der Laak, J.: 1399 H&E-stained sentinel lymph node sections of breast cancer patients: the CAMELYON dataset. *GigaScience* **7**(6) (Jun 2018)
19. Litjens, G., Sánchez, C.I., Timofeeva, N., Hermens, M., Nagtegaal, I., Kovacs, I., Hulstegen-van de Kaa, C., Bult, P., van Ginneken, B., van der Laak, J.: Deep learning as a tool for increased accuracy and efficiency of histopathological diagnosis. *Scientific Reports* **6**, 26286 (May 2016)
20. Lu, M.Y., Williamson, D.F.K., Chen, T.Y., Chen, R.J., Barbieri, M., Mahmood, F.: Data-efficient and weakly supervised computational pathology on whole-slide images. *Nature Biomedical Engineering* **5**(6), 555–570 (Jun 2021)
21. Pan, S.J., Yang, Q.: A Survey on Transfer Learning. *IEEE Transactions on Knowledge and Data Engineering* **22**(10), 1345–1359 (Oct 2010)
22. Shao, Z., Bian, H., Chen, Y., Wang, Y., Zhang, J., Ji, X., Zhang, Y.: Transmil: Transformer based correlated multiple instance learning for whole slide image classification. In: *NIPS* (2021)
23. Tsuneki, M., Abe, M., Kanavati, F.: A Deep Learning Model for Prostate Adenocarcinoma Classification in Needle Biopsy Whole-Slide Images Using Transfer Learning. *Diagnostics* **12**(3), 768 (Mar 2022), number: 3
24. Tsuneki, M., Abe, M., Kanavati, F.: Transfer Learning for Adenocarcinoma Classifications in the Transurethral Resection of Prostate Whole-Slide Images. *Cancers* **14**(19), 4744 (Jan 2022), number: 19
25. Vaswani, A., Shazeer, N., Parmar, N., Uszkoreit, J., Jones, L., Gomez, A.N., Kaiser, L.u., Polosukhin, I.: Attention is all you need. In: *NIPS* (2017)
26. Wang, Y., Li, J., Lyu, M., King, I.: Cross-media keyphrase prediction: A unified framework with multi-modality multi-head attention and image wordings. In: *EMNLP*. pp. 3311–3324. *ACL* (Nov 2020)
27. Xing, X., Chen, Z., Zhu, M., Hou, Y., Gao, Z., Yuan, Y.: Discrepancy and gradient-guided multi-modal knowledge distillation for pathological glioma grading. In: *MICCAI. Lecture Notes in Computer Science*, vol. 13435, pp. 636–646 (2022)
28. Xiong, C., Chen, H., Sung, J., King, I.: Diagnose like a pathologist: Transformer-enabled hierarchical attention-guided multiple instance learning for whole slide image classification. *CoRR* **abs/2301.08125** (2023)
29. Yu, X., Wang, J., Hong, Q.Q., Teku, R., Wang, S.H., Zhang, Y.D.: Transfer learning for medical images analyses: A survey. *Neurocomputing* **489**, 230–254 (Jun 2022)
30. Zagoruyko, S., Komodakis, N.: Paying more attention to attention: Improving the performance of convolutional neural networks via attention transfer. In: *ICLR* (2017)

31. Zhuang, F., Qi, Z., Duan, K., Xi, D., Zhu, Y., Zhu, H., Xiong, H., He, Q.: A Comprehensive Survey on Transfer Learning. *Proceedings of the IEEE* **109**(1), 43–76 (Jan 2021), conference Name: *Proceedings of the IEEE*